



Trabecular bone density distribution in the scapula relevant to reverse shoulder arthroplasty

Matt A. Daalder, MSc^a, Gabriel Venne, PhD^a, Varun Sharma, MD, FRCSC^b,
Michael Rainbow, PhD^c, Timothy Bryant, PhD^c, Ryan T. Bicknell, MD, MSc, FRCSC^{b,c,*}

^a Department of Biomedical and Molecular Sciences, Queen's University, Kingston, ON, Canada

^b Department of Surgery, Queen's University, Kingston, ON, Canada

^c Mechanical and Materials Engineering, Queen's University, Kingston, ON, Canada

ARTICLE INFO

Keywords:

Scapula
Bone density
Arthroplasty
Shoulder
Glenoid
Reverse

Level of evidence: Anatomy Study, Imaging

Background: How trabecular bone density varies within the scapula and how this may lead to more optimal reverse shoulder arthroplasty (RSA) screw placement has not been addressed in the scientific literature. The 3 columns of trabecular bone within the scapula adjacent to the glenoid fossa, one extending through the lateral border, a second into the base of the coracoid process, and a third extending into the spine of the scapula, were hypothesized to be of relatively similar density.

Methods: Two-dimensional axial computed tomography (CT) images of 19 fresh frozen cadaver specimens were obtained. Digital Imaging and Communications in Medicine (DICOM; National Electrical Manufacturers Association, Rosslyn, VA, USA) image files of the CT scanned scapulae were imported into Mimics 17.0 Materialise Software (Leuven, Belgium) for segmentation and 3-dimensional digital model generation. To determine the distribution of trabecular bone density, Hounsfield unit (HU) values in the scapulae gray value files obtained from Mimics were filtered to remove any cortical bone. HU values of 650 define the corticocancellous interface in CT image data and were considered to be cortical bone. Analyses of variance with post hoc Bonferroni tests were used to determine statistical differences between the intra- and inter-regions of bone density comparisons.

Results: The base of the coracoid process was statistically significantly less dense than the spine and the lateral border of the scapulae examined ($P < .05$).

Discussion/Conclusion: The higher-quality bone in the spine and lateral border, compared with the coracoid regions, may provide better bone purchase for screws when fixing the glenoid baseplate in RSA.

© 2018 The Authors. Published by Elsevier Inc. on behalf of American Shoulder and Elbow Surgeons.

This is an open access article under the CC BY-NC-ND license (<http://creativecommons.org/licenses/by-nc-nd/4.0/>).

Reverse total shoulder arthroplasty (RSA) is a reliable treatment option for patients presenting with a deficient rotator cuff, severe arthritis, or failed prior shoulder prostheses.^{4,8,10,11,19,20,28} Unfortunately, glenoid component loosening is a common mode of failure^{10,12,14,18,23} and has been reported as the most common need for revision surgery in RSA.¹⁴ Optimal screw positioning is important for long-term success of the prosthesis and to prevent glenoid component failure.²⁸

Several studies have investigated the effects of screw placement on baseplate fixation while taking the morphology of the scapula into account.^{8,9,11,18–20,28} These studies indicate that surgeons should attain maximum screw length, far cortical fixation, and screw placement in the best quality bone available when performing RSA.^{6,8,9,11,19,20,28} To accomplish this, information on scapular

morphology and bone quality is required; however, few studies targeting optimal screw placement have taken bone density into account.^{11,28}

Although numerous studies have aimed to characterize the osseous anatomy of the scapula, few have focused on quantitatively analyzing bone quality to suggest optimal screw placement in RSA.^{3,5,11,25,35} There are 3 columns of bone extending from the glenoid base. These 3 structures include the scapular spine, lateral border, and base of the coracoid process.^{11,19,22,28} A study conducted by DiStefano et al¹¹ determined the areas of thickest cortical bone in the scapula were present in these columns, although only a comparatively small area in the base of the coracoid is thick. This led to the question of how internal bone density varies within the scapula and how this may lead to more optimal RSA screw placement.

The aim of this study was to quantify the relative anatomic distribution of trabecular bone density in regions of the scapula adjacent to the glenoid accessible to screw fixation in RSA surgery. We hypothesized that the 3 columns of trabecular bone within the scapula adjacent to the glenoid fossa would have similar average bone density

* Corresponding author: Ryan T. Bicknell, MD, Division of Orthopaedic Surgery, Department of Surgery, Kingston General Hospital, Watkins 3, Queen's University, 76 Stuart Street, Kingston, ON K7L 2V7, Canada.

E-mail address: rtbickne@yahoo.ca (R.T. Bicknell).

and that the density within each region would be consistent throughout.

Materials and methods

Specimens and image acquisition

Fresh frozen forequarters from 19 deceased donors (8 men, 9 women, 2 unknown), with a mean age of 70 years (range, 33–98 years), were thawed, and computed tomography (CT) scanned using a Lightspeed+ XCR 16-slice CT scanner (General Electric, Milwaukee, WI, USA). The entire scapula and humerus were scanned with a tube current of 120 kVP and 100 mA, and voxel size of (0.625 mm × 0.625 mm × 0.625 mm).

Image processing

Digital Imaging and Communications in Medicine (DICOM; National Electrical Manufacturers Association, Rosslyn, VA, USA) image files of the CT-scanned scapulae were imported into Mimics 17.0 software (Materialise Software, Leuven, Belgium) for segmentation and 3-dimensional (3D) digital model generation. Segmentation was used to generate 3D tessellated surface mesh models and masks of the scapulae containing 3D voxel locations and corresponding Hounsfield units (HU). To facilitate comparison, all left scapulae were mathematically converted to right scapulae.³⁶

The trabecular and cortical bone of the scanned scapulae were isolated from other tissues, and the scapulae segmentation masks were filled to ensure all material was accounted for when the 3D digital models were created. To increase model fidelity, the segmented specimen masks and 3D models were visually inspected for any discontinuities and were further segmented until proper anatomic representation of the specimens was achieved.

We defined a previously established anatomic coordinate system to facilitate comparison across specimens.³⁴ Briefly, the coordinate frame was defined by a computer-assisted designed quadripod aligned manually to points on the supraglenoid and infraglenoid tubercles, and the trigonum spinae. The Y axis (superior-inferior) was defined by the line connecting the supraglenoid and infraglenoid tubercles, and the Z axis (medial-lateral) was defined by the line connecting the trigonum spinae to the center of the glenoid. The X axis (anterior-posterior) was defined as the axis orthogonal to the Y-Z plane. The coordinate system was then used to align the 3D surface models and corresponding voxels (Fig. 1).

Regions of interest (ROIs) within each scapula were defined and extracted for comparative analysis of the trabecular bone. The volumetric ROIs were determined based on potential RSA glenoid baseplate screw positioning. These included the base of the coracoid inferior to the suprascapular notch, the base of the coracoid lateral to the suprascapular notch, an anterior and posterior portion of the scapular spine, an anterosuperior portion of the lateral border, and an inferior portion of the lateral border. The ROIs were determined visually on the surface mesh model of each scapula displayed in MATLAB (MathWorks, Natick, MA, USA). The ROIs were bounded by X, Y, and Z coordinates, and the corresponding voxels were extracted from the segmentation masks as per defined standard protocol (Table I) and subsequently registered to the surface model to check for accuracy (Figs. 2–7).

Outcome measures

HU values in the scapula and their associated voxels were filtered to remove any cortical bone: all voxels with a HU value of 0 to 650 were kept, whereas all other HU values in the file were removed from the pool of data. HU values of 650 were chosen as

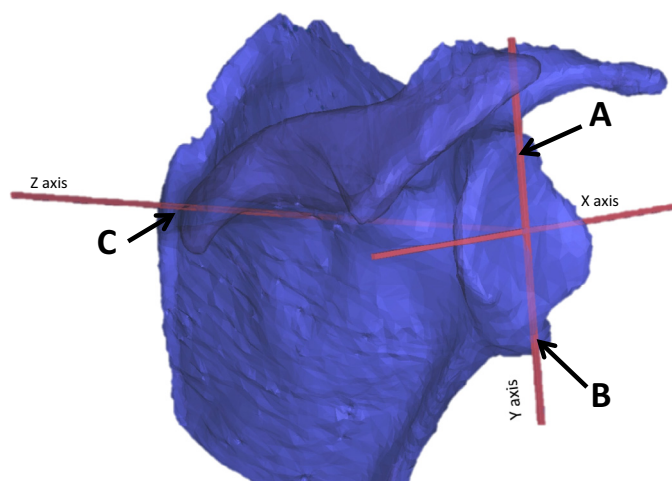


Figure 1 Quadripod oriented with respect to the supraglenoid (A) and infraglenoid (B) tubercles and the trigonum spinae (C) of a model scapula in Mimics software (Materialise Software, Leuven, Belgium). The 3 points on the quadripod define the origin of the coordinate system (near the middle of the glenoid surface), a point along the X axis (anterior to posterior) and a point along the Y axis (superior to inferior). The Z axis passes medial to lateral through the trigonum spinae.

the upper bound because studies have shown this number defines the corticocancellous interface in CT image data.^{1,13,29}

Statistical analyses

One-way analyses of variance with post hoc Bonferroni tests were used to compare the mean HU values within and between the 3 columns of the scapula. Specifically, inter-regions comparisons included the mean HU values of the coracoid ROIs, scapular spine ROIs, and lateral border ROIs. Intraregion comparisons included the anterior spine compared with the posterior portion of the scapular spine, the anterosuperior portion of the lateral border compared with the inferior portion of the lateral border, and the base of the coracoid inferior to the suprascapular notch compared with the base of the coracoid lateral to the suprascapular notch. An α value of <0.05 was considered statistically significant.

Results

Across specimens, the mean HU values of the ROI in the scapula ranged from 238.1 ± 48.0 HU to 335.2 ± 29.6 HU (Table II, Fig. 8). There were statistically significant inter-region differences between the mean HU values in the regions of interest ($P < .001$, Table III); however, there were no significant intra-region differences in trabecular bone density distribution within regions of the coracoid ($P = .99$), the lateral border ($P = .99$), or the spine ($P = .90$).

We found that regions of the coracoid were significantly less dense than all other ROIs. The superior coracoid was significantly less dense than the inferior and anterosuperior lateral border (-25.6% [$P < .001$] and -20.8% [$P < .001$]), as well as the posterior and anterior scapular spine (-29% [$P < .001$] and -23.8% [$P < .001$]). The inferior coracoid was also significantly less dense than the inferior and anterosuperior lateral border (-20.1% [$P < .001$] and -15% [$P = .004$]), as well as the posterior and anterior scapular spine (-23.7% [$P < .001$] and -18.1% [$P < .001$]). The inferior lateral border was no denser than both areas of the spine ($P = .99$), whereas the anterosuperior lateral border density was not significantly different than the posterior spine ($P = .07$) or the anterior spine ($P = .99$). There was no significant difference between the spine and lateral border ($P = .99$).

Table I
Protocol for determining regions of interest in the scapula based on global coordinate system space

Region	Min X (mm)	Max X (mm)	Min Y (mm)	Max Y (mm)	Min Z (mm)	Max Z (mm)
Coracoid Inferior	~1	Between the lateral edges of suprascapular notch and edge of glenoid.	~ 1	Inferior margin of suprascapular notch.	Medial edge of suprascapular notch.	Lateral border of the neck of the glenoid (–12).
Superior	~3	Anterior border of glenoid.	Coracoid inferior Max Y –5 mm.	Coracoid inferior Max Y +10 mm.	Between the lateral and inferior border of the suprascapular notch.	Lateral border of the neck of the glenoid (–12).
Spine Anterior	Point where the inferior margin of the spine extends from the body.	+4 of origin.	Point where the inferior margin of the spine extends from the body.	Base of the supraspinous fossa.	–40	Medial border of the neck of the glenoid at the glenoacromial notch.
Posterior	Just posterior of the posterior border of the glenoid.	Point where the inferior margin of the spine extends from the body.	Point where the inferior margin of the spine extends from the body.	Superior most y-point of the spine at Min X.	–40	Middle of the posterior border of the glenoacromial notch.
Lateral border Anterosuperior	~ –4	Anterior most point of the lateral border in the area of the infraglenoid tubercle.	~ –10 from the infraglenoid tubercle.	~ +5 from the infraglenoid tubercle.	Where the lateral border ends and subscapular fossa begins on the Min Y axis.	Lateral border of the neck of the glenoid (–10).
Inferior	Posterior most margin of the lateral border.	Anterior margin of the lateral border on the Min Y axis.	16 mm inferior to Max Y (–25 mm).	Inferior most margin of the glenoid.	Where the lateral border ends and subscapular fossa begins on the Min Y axis.	Lateral border of the neck of the glenoid (–10).

Discussion

Although we hypothesized that there were 3 columns of similarly dense trabecular bone extending from the glenoid in the scapula, our results indicate that the lateral border and spine of the scapula contain denser bone than in the base of the coracoid process. ROIs of the base of the coracoid were 15% to 25% less dense than

ROIs in the lateral border and 18% to 29% less dense compared with ROIs in the spine. As hypothesized, differences in trabecular bone density within the anatomic structures analyzed were not significant.

To our knowledge, these results constitute a new finding because no previous study has quantitatively defined the trabecular bone density in the scapula beyond the glenoid vault. However, a previous study quantitatively determined that relatively thick cortical

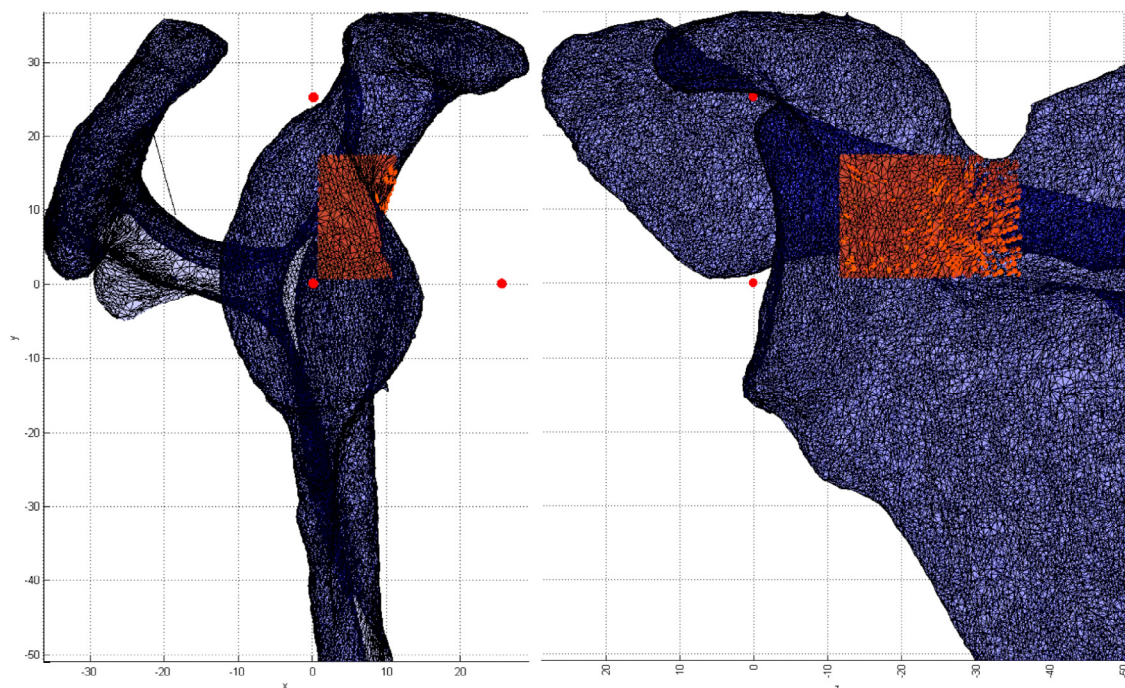


Figure 2 Regions of interest (red areas) in the inferior coracoid region inferior to the suprascapular notch, as shown in the (Left) sagittal plane and (Right) coronal plane. The 3 red dots represent the P1, P2, and P3 coordinate points from the assigned quadripod.

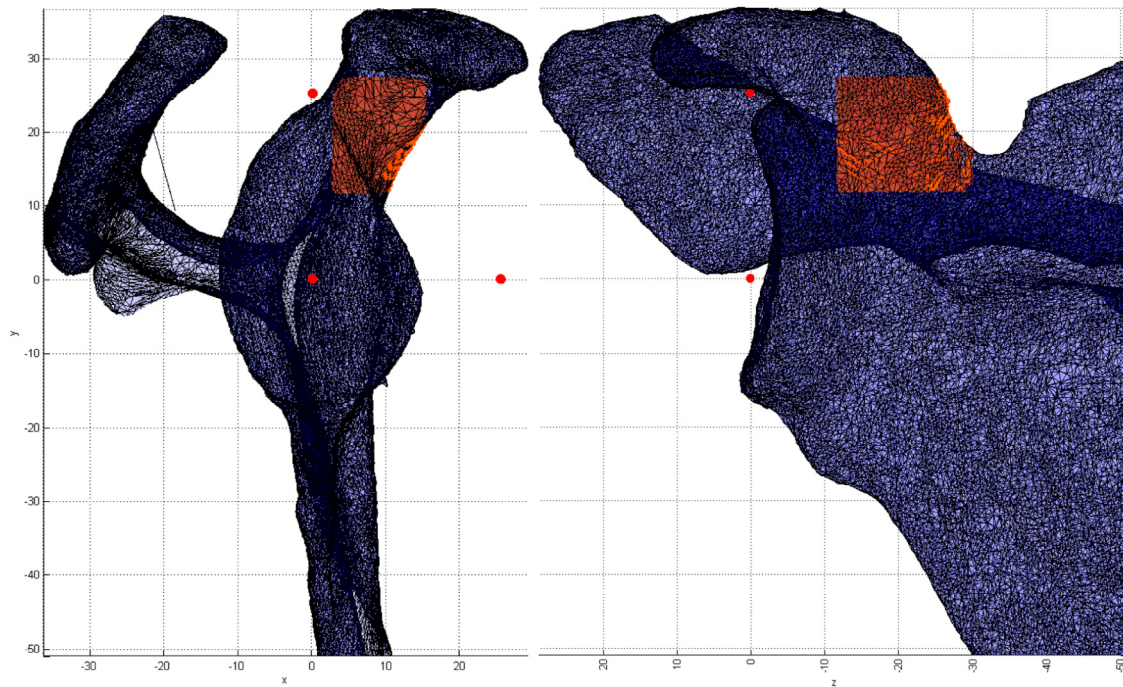


Figure 3 Regions of interest (red areas) in the superior coracoid region lateral to the suprascapular notch, as shown in the (Left) sagittal plane and (Right) coronal plane. The 3 red dots represent the P1, P2, P3 coordinate points from the assigned quadripod.

bone accessible to RSA is most prevalent in the same regions that correspond to the dense trabecular bone determined in this study: the lateral border and lateral aspect of the spine have thick bone, whereas only a comparatively small area in the base of the coracoid has thick cortical bone.¹¹ Because bone architecture responds to mechanical loading,^{7,31} the greater mechanical forces and stresses experienced during humeral abduction and anteflexion by the spine

and lateral border relative to the coracoid process could be an explanation for the spatial distribution of bone density in the scapula.^{15,24,32}

Our results should be interpreted in the context of several limitations. Our results were obtained from fresh-frozen thawed cadaveric specimens with no clear evidence of osteoarthritis. Although literature indicates that freeze-thaw cycles of fresh, untreated

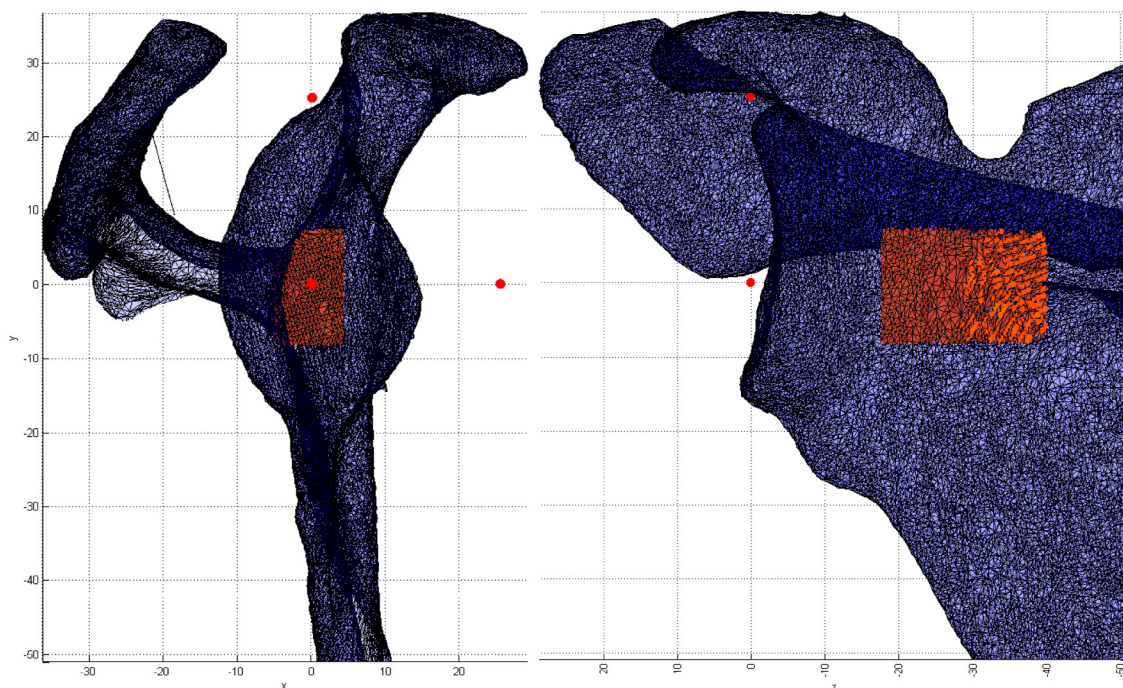


Figure 4 Regions of interest (red areas) in the anterior spine region, as shown in the (Left) sagittal plane and (Right) coronal plane. The 3 red dots represent the P1, P2, and P3 coordinate points from the assigned quadripod.

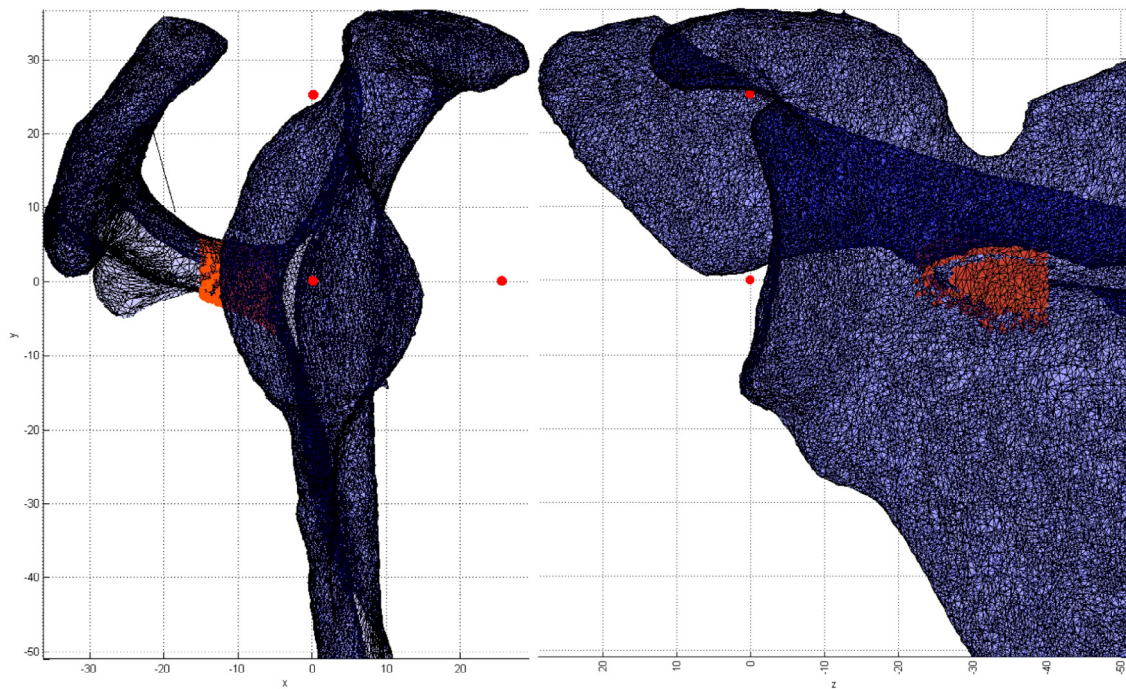


Figure 5 Regions of interest (*red areas*) in the posterior spine region, as shown in the (**Left**) sagittal plane and (**Right**) coronal plane. The 3 *red dots* represent the P1, P2, and P3 coordinate points from the assigned quadrupod.

tissues do not alter trabecular bone mechanical properties,^{16,21,26} more studies, including preoperative imaging from RSA patients would be needed to validate the bone density distribution in these patients, who often present with advanced osteoarthritis. The second part of this study aims to alleviate this and will be conducted using the methods reported and validated here to quantify the bone density distribution in the scapulae of patients selected for RSA.

Furthermore, although our study established the trabecular bone density distribution in the scapula, no biomechanical testing was done in the scapula to determine whether these distributions correlate with screw pullout strength or the integrity of baseplate fixation. However, the literature is clear: the anchorage strength of screws increases with greater trabecular bone density, regardless of bicortical, unicortical, or cancellous only fixation.^{2,27,33} Indeed,

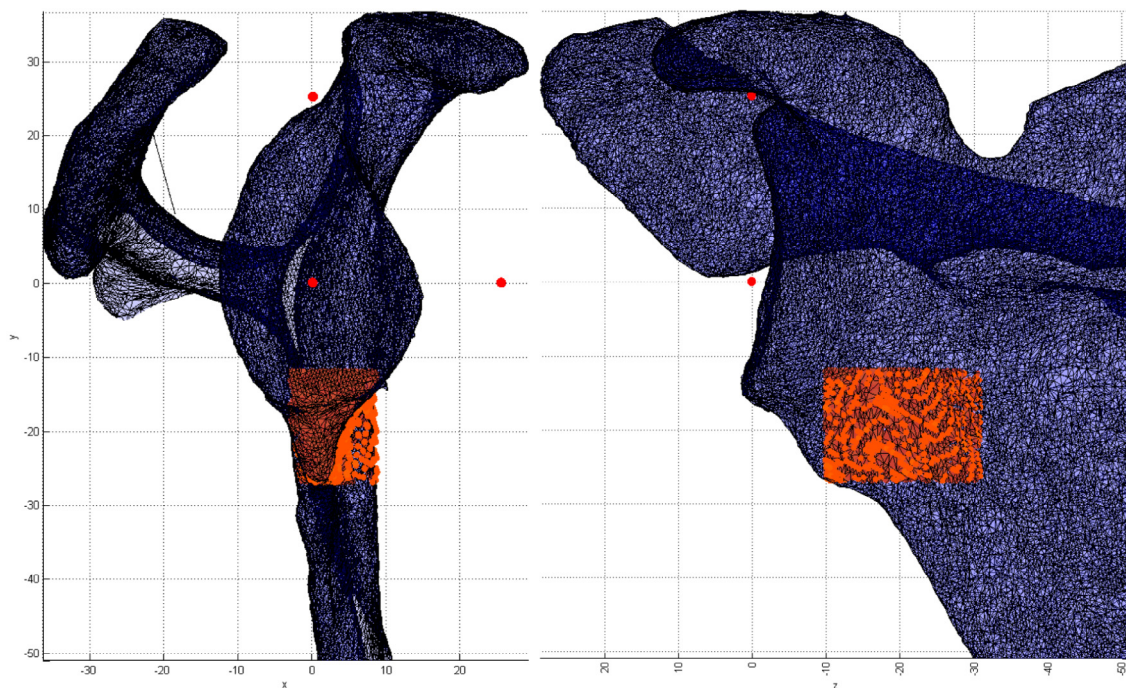


Figure 6 Regions of interest (*red areas*) in the anterosuperior lateral border region, as shown in the (**Left**) sagittal plane and (**Right**) coronal plane. The 3 *red dots* represent the P1, P2, and P3 coordinate points from the assigned quadrupod.

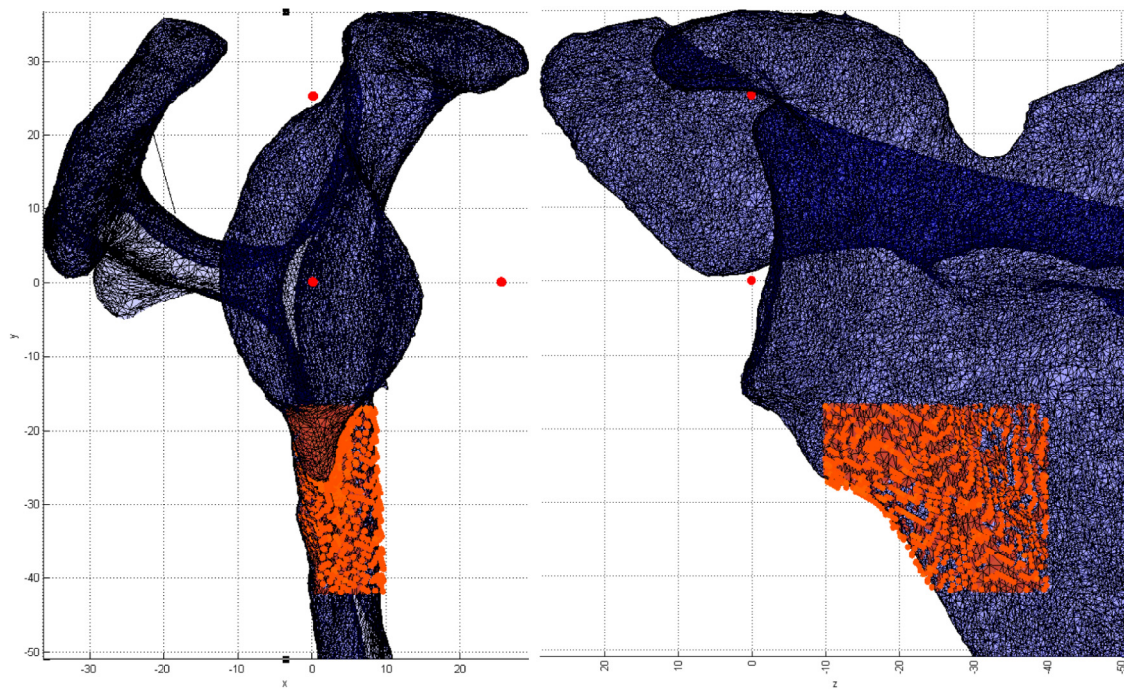


Figure 7 Regions of interest (red areas) in the inferior lateral border region, as shown in the (Left) sagittal plane and (Right) coronal plane. The 3 red dots represent the P1, P2, and P3 coordinate points from the assigned quadripod.

previous studies have determined that load to failure is less when the glenoid component is fixed to material of lesser density,⁸ and micromotion of the baseplate increases as the stiffness of the surrounding bone in which the screws are implanted decreases.¹⁸ Further biomechanical testing would have to be undertaken to verify the real-world application of this study's results.

Our approach has several potential clinical applications. The results from the intraregion comparisons indicate differences in densities between the subregions of anatomic structures in the scapula are not significant. The results of the intraregion comparisons indicate that screws aimed at the spine, lateral border, or coracoid process may not find greater trabecular bone purchase in a specific area of the respective anatomic landmark. Thus, based solely on trabecular bone density affecting screw fixation, there is increased flexibility available to the surgeon when inserting variable angle screws in each location.

The results from the inter-region comparisons suggest that the base of the coracoid is up to 29% less dense than other areas of the scapula adjacent to the glenoid, which could have meaningful clinical applications useful for optimizing glenoid baseplate design in

RSA. Notably, studies have shown that screw pullout strength decreases significantly with decreased bone mineral density^{17,30}; therefore, greater care should be taken to ensure a screw inserted in the base of the coracoid has the best mechanical advantage possible.

DiStefano et al¹¹ noted that, provided placement of other screws is not compromised, the optimal screw purchase occurs at the thickest and best cortical bone in the base of the coracoid, mainly in the inferior and slightly lateral margin of the suprascapular notch. Surgeons must therefore carefully plan the trajectory of the screw into the base of the coracoid, because there is only a small area of thick cortical bone available for screw fixation compared with the larger areas of thick cortical bone in the lateral border and spine.

Regardless, optimal screw placement is usually defined by achieving maximum screw length, far cortical fixation, and attaining screw purchase in good bone stock, defined as the densest bone possible of appropriate thickness.^{8,9,11,18-20,28} Because load to failure is less when the glenoid component is fixed to material of lesser density⁸ and micromotion of the baseplate increases as the stiffness of the surrounding bone decreases,¹⁸ surgeons are encouraged to implant screws in areas of the best bone stock where cortical fixation can also be achieved.^{8,11} Interestingly, current RSA implant designs use 4 screws that are anchored inferiorly in the lateral border, superiorly in the base of the coracoid, and anteriorly and posteriorly in the glenoid vault, but ignore the thick cortical and dense trabecular bone of the spine.

Some studies argue that the screws implanted in the glenoid are too short and anchored in bone of insufficient quality for screw fixation due to osteoarthritic deterioration and thus should not be relied on for having a major influence on baseplate fixation.^{9,20} This indicates that more efficient alternatives using long screws anchored in denser trabecular bone and thick cortical bone beyond the glenoid vault may provide optimal fixation and provides evidence for assessing the design of a baseplate geometry that emphasizes screw purchase in the lateral border and spine and carefully optimizes the trajectory of a screw implanted in the base of the coracoid.

Table II
Hounsfield unit values for regions of interest analyzed in 19 cadaveric scapulae

Region	Hounsfield units		
	Mean ± SD	Minimum	Maximum
Coracoid			
Superior	238.1 ± 48.0	191.6	364.5
Inferior	255.8 ± 31.2	207.9	332.4
Lateral border			
Anterosuperior	300.8 ± 37.9	243.8	378.0
Inferior	320.0 ± 40.0	261.7	412.9
Spine			
Anterior	312.4 ± 32.2	268.6	396.9
Posterior	335.2 ± 29.6	280.7	400.3

SD, standard deviation.

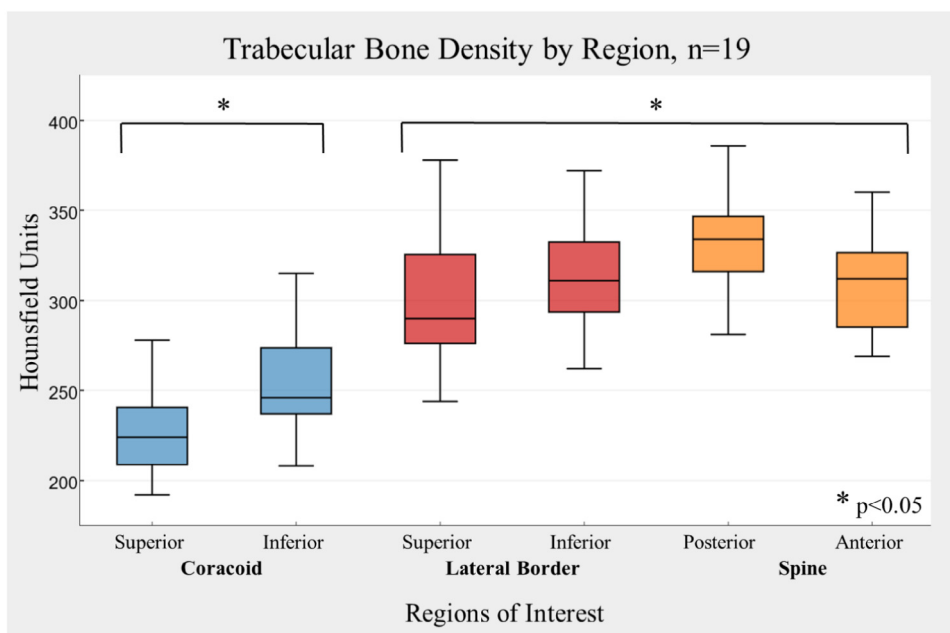


Figure 8 Box-and-whisker plots of the mean Hounsfield unit values for each region of interest in the scapula. The blue boxes represent areas of the base of the coracoid, red indicates regions of the lateral border, and orange designates regions of the scapular spine. The horizontal line in the middle of each box indicates the median, the top and bottom borders of the box mark the 75th and 25th percentiles, respectively, and the whiskers mark the 90th and 10th percentiles. **P* < .05 indicating a significant difference in mean Hounsfield unit values, wherein the base of the coracoid is less dense than all other regions of interest.

Another potential baseplate design may use 3 screws instead of the traditional 4-screw geometry, which would minimize the loss of native bone stock and allow longer screws to be inserted into the areas of greatest trabecular bone density, and bicortically into the thickest cortical bone. The configuration of such a design has been explored in the past,^{9,19,28} but no biomechanical testing has been done to date. Future steps to determine the optimal screw position in RSA should include biomechanical testing of new screw positions in the spine of the scapula, and optimal positioning of the screw in the coracoid, in both four screw and three screw baseplate configurations.

Conclusion

In our sample, the lateral border and spine of the scapula appeared to have relatively denser trabecular bone compared with the base of the coracoid process, but there was no difference in overall bone density within these anatomic structures. The higher-quality bone in the spine and lateral border compared with the

coracoid region may provide better bone purchase for screws when fixing the glenoid baseplate in RSA. The results of this research could guide future studies aimed at examining the insertion trajectories of screws and the design of the glenoid baseplate used in RSA to better integrate the anatomy of the scapula and improve implant survival.

Acknowledgment

The authors thank Heather Grant for her contributions to this manuscript, and wish to acknowledge the department of Anatomy, Rick Hunt, and Earl Dickinson for their contribution to this work.

Disclaimer

The authors, their immediate families, and any research foundations with which they are affiliated have not received any financial

Table III
P values from the inter- and intraregion mean Hounsfield unit comparisons of all regions of interest obtained from 19 cadaveric scapulae*

ROI	Coracoid		Lateral border		Spine	
	Superior <i>P</i> value	Inferior <i>P</i> value	Anterosuperior <i>P</i> value	Inferior <i>P</i> value	Anterior <i>P</i> value	Posterior <i>P</i> value
Coracoid						
Superior	—	.99	<.001	<.001	<.001	<.001
Inferior	.99	—	.004	<.001	<.001	<.001
Lateral border						
Anterosuperior	<.001	.004	—	.99	.99	.07
Inferior	<.001	<.001	.99	—	.99	.99
Spine						
Anterior	<.001	<.001	.99	.99	—	.90
Posterior	<.001	<.001	.07	.99	.90	—

ROI, region of interest.

* A *P* value of <0.05 was considered statistically significant.

payments or other benefits from any commercial entity related to the subject of this article.

References

- Aamodt A, Kvistad KA, Andersen E, Lund-Larsen J, Eine J, Benum P, et al. Determination of the Hounsfield value for CT-based design of custom femoral stems. *J Bone Jt Surg* 1999;81:1-5.
- Ab-Lazid R, Perilli E, Ryan MK, Costi JJ, Reynolds KJ. Pullout strength of cancellous screws in human femoral heads depends on applied torque, trabecular bone microarchitecture, and areal bone mineral density. *J Mech Behav Biomed Mater* 2014;40:354-61. <http://dx.doi.org/10.1016/j.jmbm.2014.09.009>
- Aggarwal A, Wahee P, Singh H, Aggarwal AK, Sahni D. Variable osseous anatomy of costal surface of scapula and its implications in relation to snapping scapula syndrome. *Surg Radiol Anat* 2011;33:135. <http://dx.doi.org/10.1007/s00276-010-0723-4>
- Alentorn-Geli E, Samitier G, Torrens C, Wright TW. Review article reverse shoulder arthroplasty . Part 2: systematic review of reoperations, revisions, problems, and complications. *Int Shoulder Surg* 2015;9:60-7. <http://dx.doi.org/10.4103/0973-6042.154771>
- Beckers A, Schenck C, Klesper B, Koebke J. Comparative densitometric study of iliac crest and scapula bone in relation to osseous integrated dental implants in microvascular mandibular reconstruction. *J Craniomaxillofac Surg* 1998;26:75-83.
- Burke CS, Roberts CS, Nyland JA, Radmacher PG, Acland RD, Voor MJ. Scapular thickness-implications for fracture fixation. *J Shoulder Elbow Surg* 2006;15:645-8. <http://dx.doi.org/10.1016/j.jse.2005.10.005>
- Carter DR, Fyhrrie DP, Whalen RT. Trabecular bone density and loading history: regulation of connective tissue biology by mechanical energy. *J Biomech* 1987;20:785-94.
- Chebli C, Huber P, Watling J, Bertelsen A, Bicknell RT, Matsen F 3rd. Factors affecting fixation of the glenoid component of a reverse total shoulder prosthesis. *J Shoulder Elbow Surg* 2008;17:323-7. <http://dx.doi.org/10.1016/j.jse.2007.07.015>
- Codsi MJ, Bennetts C, Powell K, Iannotti JP. Locations for screw fixation beyond the glenoid vault for fixation of glenoid implants into the scapula: an anatomic study. *J Shoulder Elbow Surg* 2007;16:S84-9. <http://dx.doi.org/10.1016/j.jse.2006.07.009>
- DeFranco MJ, Walch G. Current issues in reverse total shoulder arthroplasty. *J Musculoskelet Med* 2011;28:85-94.
- DiStefano JG, Park AY, Nyugen TQ, Diecherichs G, Buckley JM, Montgomery WH. Optimal screw placement for base plate fixation in reverse total shoulder arthroplasty. *J Shoulder Elbow Surg* 2011;20:467-76. <http://dx.doi.org/10.1016/j.jse.2010.06.001>
- Farshad M, Gerber C. Reverse total shoulder arthroplasty—from the most to the least common complication. *Int Orthop* 2010;34:1075-82. <http://dx.doi.org/10.1007/s00264-010-1125-2>
- Fat DL, Galvin R, O'Brien F, McGrath F, Mullett H. The Hounsfield value for cortical bone geometry in the proximal humerus—an in vitro study. *Skeletal Radiol* 2012;41:557-68. <http://dx.doi.org/10.1007/s00256-011-1255-7>
- Fevang BT, Lie SA, Havelin LI, Skredderstuen A, Furnes O. Risk factors for revision after shoulder arthroplasty. *Acta Orthop* 2009;80:83-91. <http://dx.doi.org/10.1080/17453670902805098>
- Gupta S, van der Helm FCT. Load transfer across the scapula during humeral abduction. *J Biomech* 2004;37:1001-9. <http://dx.doi.org/10.1016/j.jbiomech.2003.11.025>
- Hale AR, Ross AH. The impact of freezing on bone mineral density: implications for forensic research. *J Forensic Sci* 2017;62:399-404. <http://dx.doi.org/10.1111/1556-4029.13273>
- Hitchon PW, Brenton MD, Coppes JK, From AM, Torner JC. Factors affecting the pullout strength of self-drilling and self-tapping anterior cervical screws. *Spine* (Phila PA 1976) 2003;28:9-13. <http://dx.doi.org/10.1097/00007632-200301010-00004>
- Hopkins AR, Hansen UN, Bull MJ, Emery R, Amis A. Fixation of the reversed shoulder prosthesis. *J Shoulder Elbow Surg* 2008;17:974-80. <http://dx.doi.org/10.1016/j.jse.2008.04.012>
- Humphrey CS, Kelly JD, Norris TR. Optimizing glenosphere position and fixation in reverse shoulder arthroplasty, part two: the three-column concept. *J Shoulder Elbow Surg* 2008;17:595-601. <http://dx.doi.org/10.1016/j.jse.2008.05.038>
- James J, Allison MA, Werner FW, McBride DE, Basu N, Sutton CG, et al. Reverse shoulder arthroplasty glenoid fixation: is there a benefit in using four instead of two screws? *J Shoulder Elbow Surg* 2013;2:1030-6. <http://dx.doi.org/10.1016/j.jse.2012.11.006>
- Kang Q, An YH, Friedman RJ. Effects of multiple freezing-thawing cycles on ultimate indentation load and stiffness of bovine cancellous bone. *Am J Vet Res* 1997;58:1171-3.
- Karelse A, Kegels L, De Wilde L. The pillars of the scapula. *Clin Anat* 2007;20:392-9. <http://dx.doi.org/10.1002/ca.20420>
- Kelly JD, Humphrey CS, Norris TR. Optimizing glenosphere position and fixation in reverse shoulder arthroplasty, Part One: the twelve-mm rule. *J Shoulder Elbow Surg* 2008;17:589-94. <http://dx.doi.org/10.1016/j.jse.2007.08.013>
- Lacroix D, Murphy LA, Prendergast PJ. Three-dimensional finite element analysis of glenoid replacement prostheses: a comparison of keeled and pegged anchorage systems. *J Biomech Eng* 2000;122:430-6.
- Lehtinen JT, Tingart MJ, Apreleva M, Warner JP. Quantitative morphology of the scapula: normal variation of the superomedial scapular angle and superior and inferior pole thickness. *Orthopedics* 2005;25:481-6.
- Linde F, Sorensen HC. The effect of different storage methods on the mechanical properties of trabecular bone. *J Biomech* 1993;26:1249-52.
- Seebeck J, Goldhahn J, Städele H, Messmer P, Morlock MM, Schneider E. Effect of cortical thickness and cancellous bone density on the holding strength of internal fixator screws. *J Orthop Res* 2004;22:1237-42. <http://dx.doi.org/10.1016/j.orthres.2004.04.0>
- Stephens BF, Hebert CT, Azar FM, Mihalko WM, Throckmorton TW. Optimal baseplate rotational alignment for locking-screw fixation in reverse total shoulder arthroplasty: a three-dimensional computer-aided design study. *J Shoulder Elbow Surg* 2015;24:1367-71. <http://dx.doi.org/10.1016/j.jse.2008.11.002>
- Teo JC, Si-Hoe KM, Keh JE, Teoh SH. Relationship between CT intensity, micro-architecture and mechanical properties of porcine vertebral cancellous bone. *Clin Biomech (Bristol, Avon)* 2006;21:235-44. <http://dx.doi.org/10.1016/j.jclinbiomech.2005.11.001>
- Tingart MJ, Lehtinen J, Zurakowski D, Warner JJ, Apreleva M. Proximal humeral fractures: regional differences in bone mineral density of the humeral head affect the fixation strength of cancellous screws. *J Shoulder Elbow Surg* 2006;15:620-4. <http://dx.doi.org/10.1016/j.jse.2005.09.007>
- Turner CH. Three rules for bone adaptation to mechanical stimuli. *Bone* 1998;23:399-407.
- van der Helm FC. Analysis of the kinematic and dynamic behaviour of the shoulder mechanism. *J Biomech* 1994;27:527-50.
- Vaughn DP, Syrcle JA, Ball JE, Elder SH, Gambino JM, Griffin RL, et al. Pullout strength of monocortical and bicortical screws in metaphyseal and diaphyseal regions of the canine humerus. *Vet Comp Orthop Traumatol* 2016;6:466-74. <http://dx.doi.org/10.3415/Vcot-15-11-0192>
- Venne G, Pickell M, Pichora DR, Bicknell RT, Ellis RE. CT image registration for evaluating reverse shoulder arthroplasty placement. <https://online.boneandjoint.org.uk/doi/abs/10.1302/1358-992x.96bsupp_16.caos2014-019>; 2018, accessed July 26, 2018.
- von Schroder HP, Kuper SD, Botte MJ. Osseous anatomy of the scapula. *Clin Orthop Relat Res* 2001;(383):131-9.
- Wiest S, Maillot C, Koritke JG. Dimensions of the human scapula. *Arch Anat Histol Embryol* 1985;68:127-37.